Fast Torque Estimation of In-Wheel Parallel Flux Switching Machines for Hybrid Trucks

E. Ilhan J. J. H. Paulides
E. A. Lomonova

Eindhoven University of Technology, The Netherlands
P.O. Box 513, 5600 MB, Eindhoven,
phone: +31 40 247 5552/2310
fax: +31 40 243 4364
e-mail: e.ilhan@tue.nl

***Abstract*—Recently, parallel flux switching machines (PFSM) have come forward as a promising candidate for hybrid and electrical truck applications due to their high power density. Torque calculations, i.e cogging and electromagnetic, are important features of these machines. However, they require a finite element model (FEM) with a long simulation time, especially for transient analyses. This paper explains how the simulation time can be minimized by employing a torque superposition principle.**

***Index Terms*—Cogging torque, electromagnetic torque, parallel flux switching, superposition principle.**

I. Introduction

In the coming years, electrical vehicles will take their place in the automotive market as a result of the desire to increase sustainable transportation solutions [1]. Before mass introduction of electrical vehicles, a transitional period will take place where hybrid cars will dominate the market. To date, most of the research and development has been devoted to passenger cars. However, a very important application area has attained significantly less attention, namely the truck industry. These applications are usually investigated from an energy storage and/or management point of view, with very little attention to the traction motor [2]- [5]. Although an improved efficiency arguably does add very little to the total power train efficiency, it does minimize the heat generation of the electrical machine which either reduces the thermal stresses (increased lifetime) or the required volumetric envelope (increased torque density). Typical traction motor topologies used by the automotive industry today are three-phase asynchronous machines, however slowly these are replaced by permanent magnet synchronous machines (PMSM) and switched reluctance machines (SRM) mainly due to their advantages in torque density and efficiency. Considering the heavy-duty transportation industry, e.g. delivery trucks with in-wheel traction machines, there is a recent trend to search for alternatives which are even more efficient in terms of power and volume. Especially for in-wheel traction machines, it is an important issue to keep a balance between the unsprung mass and efficiency [6]. Parallel flux switching machines (PFSM) try to provide a solution by combining the advantages of the PMSM and SRM.

Due to the nonlinear characteristics of this class of machines, see Section 2, it is time consuming to determine the key electrical machine design parameters. To date, FEM seems to be the only used method [7]-[9]. However it takes a long calculation time, especially for transient analyses, which is already necessary for a simple torque calculation. An alternative is the superposition principle, as proposed in this paper, which is applied for the first time to this class of machines.

II. Parallel Flux Switching Machines (PFSM)

The PFSM is a comparably new electrical machine for the automotive sector. The classification of this machine is not straightforward. Energy sources are placed in stator, instead of traditionally separate frames as used in Brushless DC machines (BLDC). Like in BLDCs, PMs as well as excitation windings are used as flux sources. They should guide the flux in such a way to minimize the equivalent reluctance and maximize torque. Although from a construction point of view PFSM mainly resembles SRM, however if a sinusoidal (armature) current is regarded the PFSM can also be classified as a Brushless PM AC motor (BLAC). The main difference between BLAC and PFSM is the mechanism responsible for the flux polarity switch [10]. For the BLAC there is only one mechanism, which is the change of rotor position from N to S pole, and for the PFSM there are two mechanisms corresponding to

zero armature flux linkage, PM-rotor tooth and PM-rotor tooth slot alignments as seen in Fig. 1.

With the absence of energy sources from rotor, the need for brushes is eliminated. Additionally, PFSM has the theoretical advantage of high speed capability together with a high torque density. Although, currently there is no data available in literature for the PFSM regarding the torque density values, it must be noted that the torque density levels compared to PMSM could be slightly lower due to the decreased armature winding space. However, the copper loss is up to four times lower than compared to a standard machine with the same size and with an increased iron loss [11].

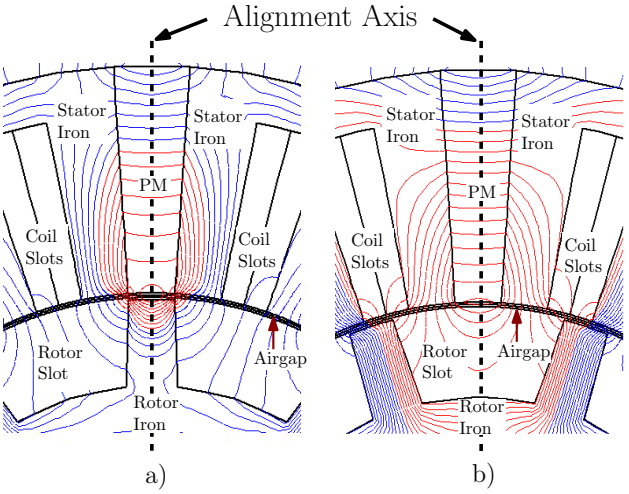

Fig. 1. Zero flux linkage positions of the PFSM (a) PM - rotor tooth alignment (b) PM - rotor tooth slot alignment.

It was mentioned that the excitation field can be produced either with field windings or PMs. On one hand, with the use of field windings high material costs and attraction forces due to the PMs can be avoided and additionally a field control would be possible. On the other hand, extra costs could appear due to the increased energy use, power electronics, control, and thermal issues. If efficiency wants to be maximized, the excitation field is most likely to be supplied by PMs, where the material selection is crucial for automotive application. In general, rare earth magnets have higher energy density compared to cheaper ferrite magnets, which results in a higher excitation flux per meter axial length and lower magnetic reaction (assuming a constant current). However if the flux weakening mode is regarded, more current density is required to achieve the same flux output for rare earth magnets due to low armature reactance [12]. Although the method proposed in this paper is applicable for both field creation techniques, for understanding purposes, the focus is

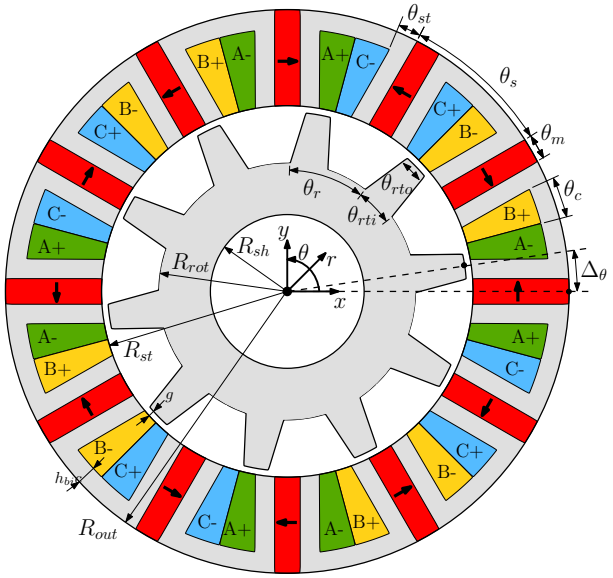

Fig. 2. Conceptual design of a 12/10 pole FSPMM.

set on the flux switching permanent magnet machine (FSPMM) as the representative of the PFSM class. The cross section of the machine is presented in Fig. 2.

A. Working Principle

For an AC machine operation, there has to be a rotating magnetic field, which can be represented as following:

$$B = B_{max} \cdot e^{jwt}, \tag{1}$$

with w angular speed of the energy source.

The rotating magnetic field can be decomposed into two alternating fields with a 90° shift:

$$B_{max} \cdot e^{jwt} = B_{max} \cdot (\cos wt + j \sin wt). \tag{2}$$

This basic principle is also valid for the PFSM. One of the two necessary alternating fields is created by the PMs (or DC windings). Although PMs are stationary, due to the rotation of the rotor, armature flux changes both in its amplitude and polarity. This results in a bipolar flux linkage between stator and rotor. Consequently, the bipolar flux creates an alternating field in the armature windings. This field is orthogonal to the alternating field in the armature windings, which is created by the sinusoidal AC current.

In order to show this relationship more clearly, the machine can be represented with simple elementary cells in rectangular coordinates due to the high number of stator/rotor pole combination. The stator consists of twelve elementary cells with an example given in Fig. 3, whereas the rotor of ten identical cells. The basic principle of flux switching in one elementary cell occurs

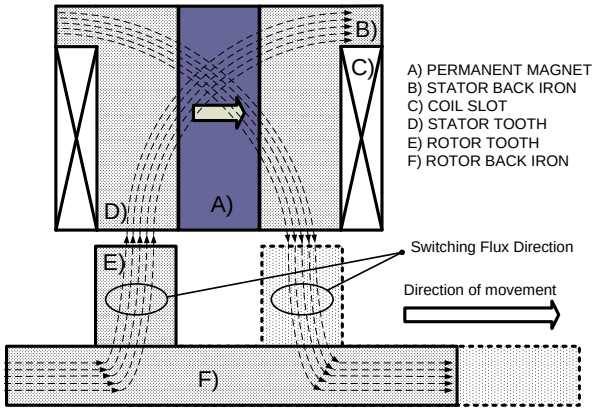

Fig. 3. Working principle of the FSPMM on the elementary cell.

due to the movement of the rotor. As shown in Fig. 3, the flux lines switch direction in the next rotor position. The resulting bipolar flux linkage is the phase flux linkage of the coil which surrounds the PM.

This bipolar flux linkage gives an increase in the energy utilization, which depends on the total change of the armature flux linkage. The increased energy use inside the machine occurs, because each coil in one elementary cell spans one of the alternating poles and a pair of laminated stator teeth. For rotary machines, this leads to a parallel magnetic coupling of energy sources (magnets and coils for the FSPMM); therefore the machine class is referred as parallel flux switching machine. Additionally, the placement of magnets leads to a prebiased structure, resulting the motor to start-up directly at saturation of the soft magnetic materials B-H curve (μ_{max}) and operating continuously near the saturation region. This point in the soft-magnetic material magnetization curve represents the maximum change in co-energy ($\frac{\partial W_c}{\partial \theta}$), resulting in a high starting torque. However, it must be noted that saturation limits the applicable (semi-)analytical modeling approaches, since it introduces a highly nonlinear behaviour [15]. The effect of saturation will be discussed in section 3 more detailed.

B. Machine Comparison

A general comparison among different machine classes is presented in Table 1 [16] with the cross sections shown in Fig. 4. In this table, two different types of PMSM are considered, the double salient permanent magnet (DSPM) and BLAC machine. The main difference between these subclasses is the placement of the PMs. On one hand the PMs are located in the stator back iron

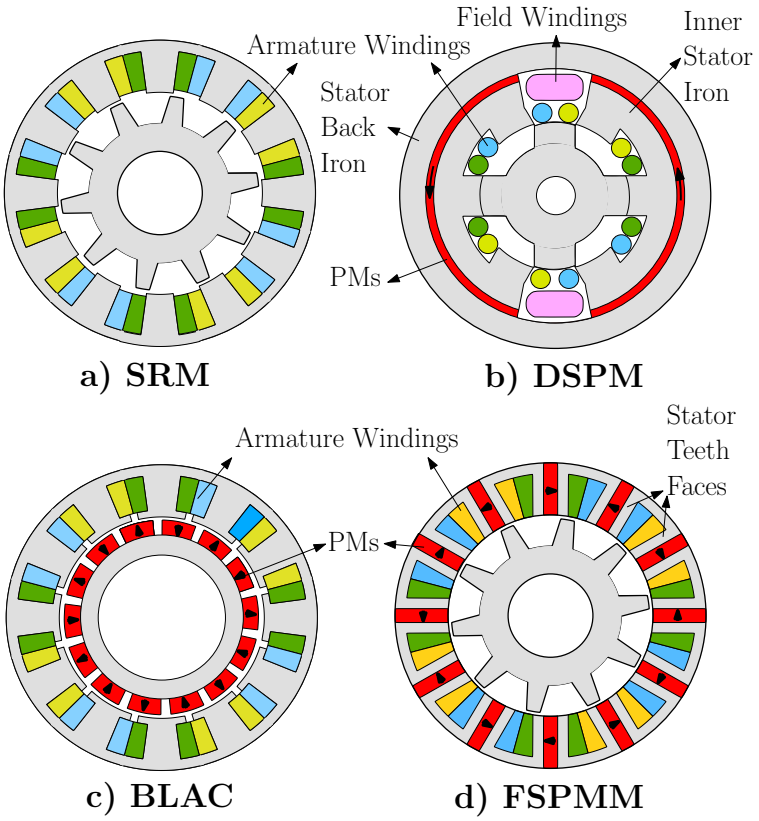

Fig. 4. Compared machine topologies.

of the DSPM similar to the FSPMM structure. On the other hand, they are placed in the rotor part for the BLAC machines leading to a lower speed operation due to the increased rotor inertia.

The operation of an electrical machine can be represented in a voltage-current, flux-current or torque-speed characteristic, i.e. energy conversion loop of the machine's operation. Electrical machines motoring in forward direction with unipolar phase flux linkage operate only in the first quadrant of the voltage-current characteristic. Some machines (e.g. DSPM) also make use of the second quadrant, where they can brake additionally in forward direction due to the bipolar current capability. The bipolar phase flux linkage enables the FSPMM and the BLAC machine the benefit to use all four quadrants of the energy conversion loop, which is the reason for the high energy utilization.

As mentioned before, the significant advantage of the FSPMM is that the PMs are situated in the stator instead of the rotor, which leads to a relatively low demagnetization probability compared to the PMSM (e.g. Brushless AC). Additionally, since the rotor is composed only of laminated ferromagnetic material, it is easier to construct and the machine requires less volume

TABLE I
COMPARISON OF MACHINE TYPES USED IN AUTOMOTIVE INDUSTRY

	SRM	**DSPM**	**BLAC**	**FSPMM**
Flux Linkage	Unipolar	Unipolar	Bipolar	Bipolar
Energy Source	Coils	Coil + Magnet in stator back iron	Coil + Magnet in rotor	Coil + Magnet in stator teeth faces
Speed Depend.	Time const.	Time const.	PM mount.	Time const.
Rotor Inertia	Low	Low	Medium / High	Low

TABLE II
LIST OF SYMBOLS

T	Torque	N m
W	Energy	J
r	Radial position (normal direction)	m
θ	Angular position (tangential direction)	degree
z	Axial position (longitudinal direction)	m
Δ	Relative position between stator and rotor	degree

giving a higher torque density. In flux weakening mode, the machine is capable to reach relatively high speeds, such as up to 50.000 rpm for a single phase 3 kW machine with a 30 mm rotor diameter [11].

III. TORQUE CALCULATIONS

In this section, the following parts explain the logic leading to the machine model reduction using the superposition principle.

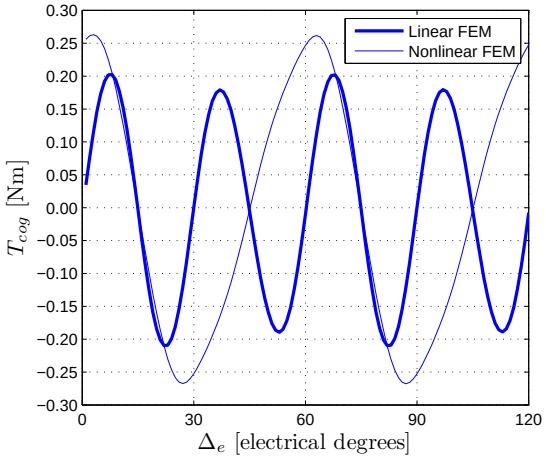

Fig. 5. Cogging torque comparison for the nonlinear and linear cases for only 2 periods.

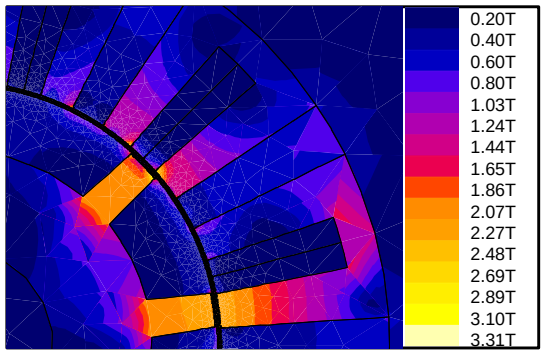

Fig. 6. Magnetic flux density distribution inside FSPMM in the presence of only two alternate teeth.

A. Saturation Effect

In sections 1 and 2, one important aspect of the PFSM was mentioned, i.e. highly saturated nature. Based on the presence of this characteristic, two different cases are created for the FSPMM example, the linear and nonlinear. Because there is an expected difference in the electromagnetic torque, the first emphasize is given to the cogging torque for the comparison.

In order to show it more clearly, only two periods of cogging torque are investigated for both linear and nonlinear cases in Fig. 5. There are two significant differences: The resulting graph from the nonlinear case clearly shows less fluctuations and exhibits higher maxima in both directions.

As for the first difference, for one total electrical cycle of 360°, there are 6 torque periods for the nonlinear case where a nonlinear B-H curve characteristic is considered. The periods correspond to the rotor tooth tip-stator tooth tip alignments during the rotor's 36° mechanical movement. Due to the pre-biased structure of the machine, the rotor pole number of the FSPMM corresponds to the rotor teeth number, which are in a sense analogue to the PMs in a BLAC machine. This pre-biased structure causes the FSPMM to operate around the knee point of the soft magnetic material's B-H curve.

B. Implementation of Superposition Principle

Saturation in the teeth tips shown in Fig. 6 causes the difference in the number of oscillations within the same periodicity of cogging torque. The oscillation clearly decreases in the nonlinear case due to the saturation, while a periodicity of 60° electrical is kept constant. To investigate this decrease in oscillations, the analysis of the whole machine is reduced to the torque calculation

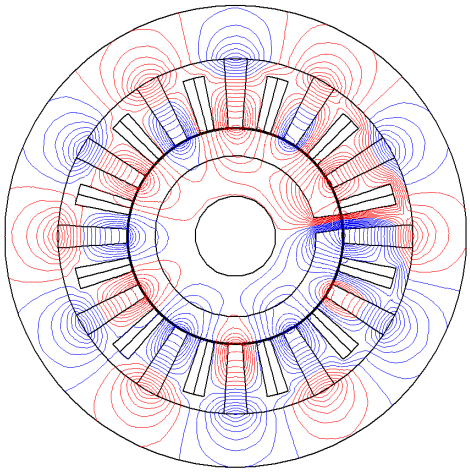

Fig. 7. Open-circuit flux distribution inside FSPMM in the presence of only one tooth.

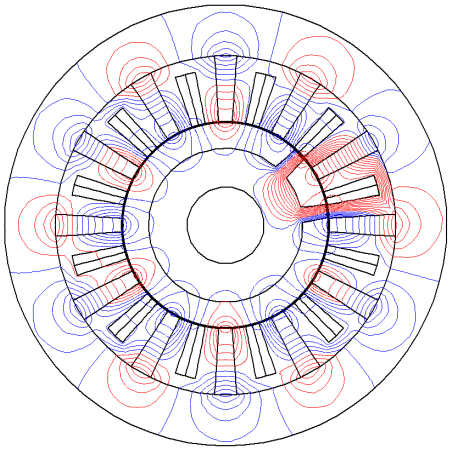

Fig. 8. Open-circuit flux distribution inside FSPMM in the presence of only two alternate teeth.

acting on a single tooth. The idea is to calculate the total torque of the machine using the superposition principle presented in [13], where this principle was applied to the PMs in the rotor of a BLAC machine.

In general, torque expression can be expanded in the following series:

$$T = \sum_{i=1}^{\infty} T_i \sin(iN\Delta_\theta), \tag{3}$$

where N is the least common multiple between the stator slot number and pole number, T_i is the amplitude of the i^{th} harmonic, and Δ_θ the mechanical angle between stator and rotor [14]. For the FSPMM, the pole number is the equivalent of the rotor teeth number. The periodicity of torque is $360/N$ in electrical degrees, which gives 6 periods for the investigated 12/10 pole machine for one electrical cycle.

For the implementation of the superposition method, two different approaches are regarded regarded: one tooth and two teeth methods. In the first one, the rotor geometry is reduced from ten to one tooth, as illustrated in Fig. 7. Following the results, which will be discussed in next section, the tooth number is increased to two teeth, as illustrated in Fig. 8.

IV. Results

The superposition method can be applied both to analytically derived and numerically solved torque calculations. If we consider the numerically derived results from FEM in Fig. 9 for one tooth, it shows that this is not satisfactory yet due to the fractional 12/10 pole combination of the investigated machine. Fig. 10 explains the reason for this result, where harmonic spectrum of the superposition methods used are shown. The one tooth approach does not follow quite the harmonic pattern of the machine torque with ten teeth. The non-integer ratio causes that not all the harmonics from the investigated one tooth approach contribute to the superimposed result. The peak in the harmonic spectrum is reached at 400 Hz, as expected. For one electrical cycle of $360°$, the machine has to rotate physically $36°$ with a speed of 400 rpm. Therefore, it takes 0.015 s. until all the samples (cogging torque values) for the fast Fourier transform are calculated. Because the torque period is $60°$ electrically, it is $0.015/6$s, which results accordingly the 400 Hz torque frequency. The harmonic analysis is realized using Fast Fourier Transform with a sampling frequency of 6666 Hz and a number of 100 samples. Due to the rules of signal processing, not to lose any information during transformations, the harmonic spectrum ends at the half of the sampling frequency.

Following the unsatisfactory results from the one tooth method, the approach is extended to the two alternate teeth. The advantage of this approach is that a return path for the flux lines is defined to derive more realistic results. These flux lines can be seen clearly in the open circuit distribution of Fig. 8, compared to Fig. 7.

In the two teeth approach the numerical torque results are superimposed instead $36°$ over $72°$ mechanical movement due to the relative position of the rotor teeth. The results in Fig. 9 for the two teeth approach clearly show an agreement for the cogging torque in (a) and match perfectly with the rated torque output resulting from the electromagnetic torque in (b).

All the FEM simulations with the one tooth and two teeth models are realized using the full machine model.

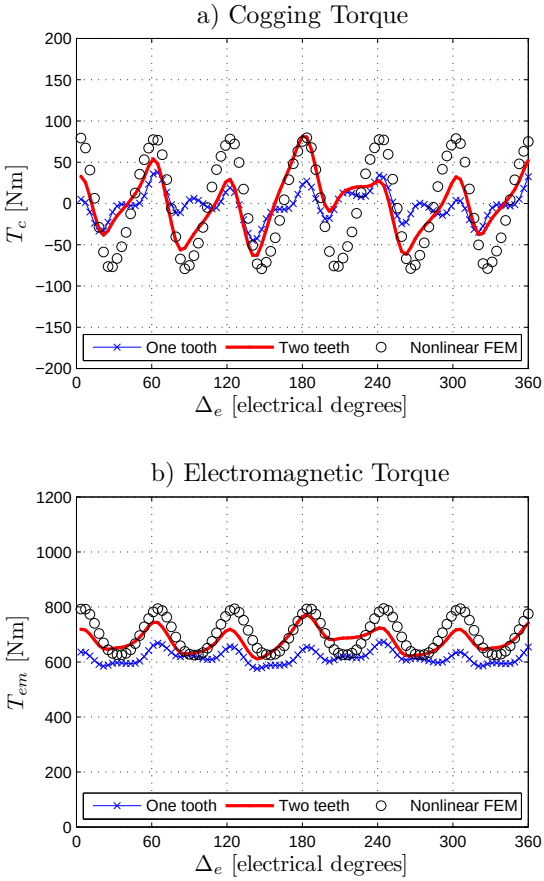

Fig. 9. Verification of superimposed torque calculations from one tooth and two teeth for a) open-circuit analysis in the nonlinear model and b) armature reaction analysis in the nonlinear model.

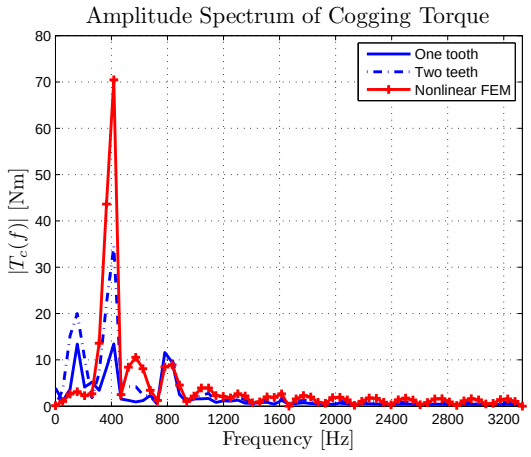

Fig. 10. Harmonic analysis of the cogging torque for the one tooth and two teeth superposition methods together with the nonlinear machine behaviour.

It is not possible to construct a half model with these properties due to the boundary condition problems. If the simulation time for torque calculation is compared with the proposed method (FEM+Matlab code) to the FEM only results, a decrease of approximately three times is achieved.

V. Conclusions

Flux switching machines are a very promising alternative to existing traction machine in the automotive industry. Their prebiased structure due to the placement of magnets into the stator leaves the rotor part suitable to reach higher speeds (only limited by rotor surface speed). In order to explain its advantages more precisely and prevent confusion, a separate section in this paper is devoted to the explanation of the working principle of the PFSM. Additionally a comparative analysis to alternative machine topologies has been presented for variable speed applications.

Due to the double salient structure and nonlinearities of the FSPMM, most researchers in this area prefer FEM for the investigation of this machine. The regarded 12/10 pole FSPMM exhibits only half machine periodicity resulting in a large FEM model and consequently long computation time, especially in the transient 2D analysis for torque calculations. This paper proposed to simplify the machine model geometrically using the superposition principle for torque calculations, which resulted in a dramatic decrease of the total simulation time for the transient analysis.

A detailed analysis of the cogging torque inside the FSPMM is given. The analysis of the different behaviours for the linear and nonlinear cases, provided the idea of using the superposition principle for fast torque estimation for this class of machines. After careful consideration of two proposed techniques, one tooth and two teeth approach, it was decided that the latter one gives more satisfactory results due to the closing of flux paths. The proposed technique is not only suitable to be used in conjunction with the proposed numerical technique but also with (semi-)analytical modeling techniques. The machine model is simplified in the rotor geometry as two teeth instead of ten, which saves a lot of computational time.

References

[1] Associated Press, "Nissan to produce electric cars in 2012", *MSNBC News*, June, 23 2009.

[2] A. Taghavipour, A. Alasty, and M.F. Saadat, "Nonlinear Power Balance Control of a SPA hydraulic hybrid truck", *Advanced Intelligent Mechatronics, 2009. AIM 2009. IEEE/ASME International Conference on*, pp. 805-810, July. 2009.

TABLE III
FSPMM PARAMETERS

N_{ph}	Number of phases	3
N_r	Rotor pole number	10
N_s	Stator pole number	12
R_{out}	Outer radius	45 cm
R_{st}	Stator radius	27.5 cm
R_{sh}	Shaft radius	10.2 cm
R_{rot}	Rotor radius	20.4 cm
R_{ag}	Center of airgap radius	27.25 cm
L_a	Axial length	25 cm
g	Airgap	0.5 cm
h_{bi}	Stator back-iron thickness	3.6 cm
θ_s	Angular stator width	$360°/N_s$
θ_m	Angular magnet width	$\theta_s/4$
θ_c	Angular coil width	$\theta_s/8$
θ_{st}	Angular stator tooth width	$\theta_s/4$
θ_r	Angular rotor width	$360°/N_r$
θ_{rto}	Angular rotor tooth outer width	θ_{st}
θ_{rti}	Angular rotor tooth inner width	$1.5\ \theta_{rto}$
Δ_θ	Mechanical displacement	θ
Δ_e	Electrical displacement	Δ_θ/N_r
N	Number of turns per phase	72
B_{rem}	Remanent flux density of permanent magnet	1.2 T
B_{sat}	Saturation level of soft mag. mat. (Magnet-iron)	2.15 T
μ_{pm}	Relative permeability of permanent magnet	1.05
μ_{max}	Magnet-iron maximum relative permeability	7000
μ_{ini}	Magnet-iron initial relative permeability	1273
I	Phase current (rms)	33 A
T	Rated torque	660 Nm
w_m	Rated speed	400 rpm

[3] C. Rudolph, "Hybrid drive system of an industrial truck using a three-phase DC-DC converter feeding ultra-capacitors", *Power Electronics and Applications, 2009. EPE '09. 13th European Conference on*, pp. 1-10, October 2009.

[4] L. Boulon, D. Hissel, M. Pera, O. Pape and A. Bouscayrol, "Energy based modeling of a 6-wheel drive hybrid heavy truck", *Vehicle Power and Propulsion Conference, 2009. VPPC '09. IEEE*, pp. 1316-1321, September 2009.

[5] L. Youxin and L. Degang, "The Elite Multi-parent Crossover Evolutionary Optimization Algorithm to Optimum Design of Automobile Gearbox", *Artificial Intelligence and Computational Intelligence, 2009. AICI '09. International Conference on*, pp. 545-549, November 2009.

[6] J.J.H. Paulides, E.V. Kazmin, B.L.J. Gysen and E.A. Lomonova, "Series Hybrid Vehicle System Analysis Using an In-Wheel Motor Design", *IEEE VPPC 2008 Conference*, China, September 2008.

[7] H. Pollock, C. Pollock, R.T. Walter and B.V. Gorti, "Low cost, high power density, flux switching machines and drives for power tools", *Artificial Intelligence and Computational Intelligence, 2009. AICI '09. International Conference on*, pp. 1451-1457, vol.3, October 2003.

[8] W. Hua, Z.Q Zhu, M. Cheng, Y. Pang and D. Howe, "Comparison of flux-switching and doubly-salient permanent magnet brushless machines", *Electrical Machines and Systems, 2005. ICEMS 2005. Proceedings of the Eighth International Conference on*, pp. 165-170, vol.1, September 2005.

[9] N.S. Lobo, E. Swint and R. Krishnan, "M-Phase N-Segment Flux-Reversal-Free Stator Switched Reluctance Machines", *Industry Applications Society Annual Meeting, 2008. IAS '08. IEEE* , pp. 1-8, October 2008.

[10] A. Zulu, B.Mecrow and M. Armstrong, "A Wound-Field Three-Phase Flux-Switching Synchronous Motor with All Excitation Sources on the Stator," in *IEEE Energy Conversion Congress and Exposition (ECCE).2009,San Jose, California, USA*, 2009, pp. 15021509.

[11] S. E. Rauch and L. J. Johnson, "Design principles of Flux-switch alternators. Power Apparatus and Systems, Part III.", *Transactions of the American Institute of Electrical Engineers*, 74(3):1261-1268, January. 1955.

[12] Y. Amara, E. Hoang, M. Gabsi, M. Lcrivain and S. Allano, "Design and comparison of different flux-switch synchronous machines for an aircraft oil breather application," in *European Transactions on Electrical Power*, 2005, vol. 15, no: 6, pp. 497511.

[13] Z. Zhu, S. Ruangsinchaiwanich, Y. Chen, and D. Howe, "Evaluation of superposition technique for calculating cogging torque in permanent-magnet brushless machines," *Magnetics, IEEE Transactions on*, vol. 42, no. 5, pp. 15971603, May 2006.

[14] Z. Zhu, S. Ruangsinchaiwanich, and D. Howe, "Synthesis of cogging torque in permanent magnet machines by superposition," in *Power Electronics, Machines and Drives, Second International Conference on (Conf. Publ. No. 498)*, vol. 2, March-April 2004, pp. 828833 Vol.2.

[15] E. Ilhan, B. Gysen, J. Paulides, and E. Lomonova, "Hybrid analytical model for flux switching permanent magnet machines", *Magnetics, IEEE Transactions on*, vol. 46, no. 6, June 2010.

[16] R.P. Deodhar, S. Andersson, I. Boldea, and T.J.E. Miller, "The flux-reversal machine: a new brushless doubly-salient permanent-magnet machine.", *Industry Applications, IEEE Transactions on*, 33(4):925-934, July/August 1997.